frontiers | Frontiers in Materials

TYPE Original Research
PUBLISHED 04 January 2023
DOI 10.3389/fmats.2022.1105351

OPEN ACCESS

EDITED BY
Xiangchen Meng,
Harbin Institute of Technology, China

REVIEWED BY
Rong Xue,
Shaanxi University of Science and Technology, China
Shang Wang,
Harbin Institute of Technology, China

*CORRESPONDENCE
Dongsheng Yang,
yangds2021@hotmail.com
Yilong Huang,
huangyilong-de@outlook.com

SPECIALTY SECTION
This article was submitted to Structural Materials, a section of the journal Frontiers in Materials

RECEIVED 22 November 2022
ACCEPTED 19 December 2022
PUBLISHED 04 January 2023

CITATION
Yang D and Huang Y (2023), Study of the properties of high silicon aluminum alloy by laser welding.
Front. Mater. 9:1105351.
doi: 10.3389/fmats.2022.1105351

Study of the properties of high silicon aluminum alloy by laser welding

Dongsheng Yang* and Yilong Huang*

Guobo Electronics Co., Ltd., Nanjing, China

High silicon aluminum alloy is a kind of high-performance electronic packaging material, due to its excellent thermal conductivity, low thermal expansion coefficient, and low density. The heat affected zone (HAZ) of conventional welding techniques is too wide to weld the high silicon aluminum alloy, as wide HAZ will improve risk of cracking. Laser welding with narrow HAZ, high joint strength, and good morphology, has been considered as a promising method to weld high silicon aluminum alloy. Herein, the surface morphology, microstructure, and microhardness of laser welding joint between Al-50wt.%Si and Al-27wt.%Si alloys were investigated. It has been found that welding speed at 3 mm–5 mm/min can significantly reduce the hydrogen pores and cracks in laser welding joints. Also, the key paraments of laser welding to control the quality of joints are power and pulse width, while the former one is mainly controlling the joint width and the latter one is significantly changing the joint depth. Along the horizontal direction of laser welding joints, the microhardness increases firstly and then decreases, with the highest microhardness of 167 HV in the weld zone. Because the laser welding method could produce uniform microstructure of joints, the microhardness of joints is uniform along the longitudinal direction. The tensile properties of welding samples are almost the same with the properties of the Al-50wt.%Si base materials.

KEYWORDS

laser welding, high silicon aluminum alloy, heat affected zone, microhardness, tensile property

1 Introduction

For modern electronics, e.g., high-power devices, there is an urgent requirement of rapid and effective heat dissipation substrate. To achieve this requirement, the substrate materials need to have high thermal conductivity more than 100 W m^{-1}·K^{-1}, and their coefficient of thermal expansion (CTE) need to match that of semiconductor materials, such as Si and GaAs (about 5 K^{-1}–9 K^{-1} × 10 K^{-1}–6 K^{-1}), and they are expected to have low density (less than 3 g cm^{-3}). The density of high silicon aluminum alloys is between 2.3 g cm^{-3} and 2.7 g cm^{-3}, and the CTE of high silicon aluminum alloys is between 4.1 K^{-1} × 10^{-6} K^{-1}–23.6 K^{-1} × 10^{-6} K^{-1}, and their conductivity is between 101 W m^{-1}·K^{-1}–126 W m^{-1}·K^{-1}. Increasing the silicon content can significantly reduce the density and the CTE of the alloy materials, but slight conductivity loss. Thus, the high silicon aluminum alloys are becoming attractive materials, especially in aerospace and advanced packaging fields.

So far, the high silicon aluminum alloys can be produced by smelting and casting process, powder metallurgy process, and jet deposition process. At present, smelting and casting process is a common method for manufacturing most alloys. It has the characteristics of low equipment requirements, simple process, low cost, and large-scale

industrial production. However, most of the high silicon aluminum alloys for electronic packaging prepared by this process have serious defects, as the size of the primary silicon in the casting microstructure is large and the solidification microstructure segregation is serious (Kun et al., 2012; Zhang et al., 2015). The preparation of high silicon aluminum alloys by powder metallurgy process is to mix aluminum powder and silicon powder in a certain proportion, and then through the process of mixing, pressure, and gas extraction, finally high density and high-quality high silicon aluminum alloys can be obtained. High silicon aluminum alloys with different silicon content can be achieved by adjusting the ratio of silicon to aluminum (Zhong et al., 2010; Liu et al., 2012). The jet deposition method is a comprehensive processing method, which combines the characteristics of rapid solidification and semi-solid processing (Chen et al., 2014).

Recent years, the friction stir welding (Meng et al., 2021), electron beam welding (Wu et al., 2006; Jia et al., 2011; Aktarer et al., 2015), and laser welding (Kutsuna et al., 2003; Quazi et al., 2015) were applied to join aluminum alloy materials. Among these methods, the laser welding is the most promising one, because it is an efficient and precise welding method using high energy density laser. The laser welding of high silicon aluminum alloy has the advantage of high-power density, high depth-to-width ratio, high speed, narrow heat affected zone (HAZ), less deformation, high joint strength, and good surface morphology (Zhao et al., 2014; Wang et al., 2021a; Hou et al., 2021). To date, studies about high silicon aluminum alloys by laser welding are mainly focused on the scheme for reducing the porosity and cracking of the welding joints, which are the most common welding defects in the joints and will significantly reduce the mechanical strength of the joints (Hu et al., 2021). It was found that defect formation during laser welding process is influenced by not only welding parameters, but also alloying compositions (Abbaschian and Lima, 2003). Zhao et al. (2014) studied the effect of Si content on laser welding performance, and the results suggested that in the low Si content alloy the residual eutectic phases exist as particles at the grain boundary, so cracking behaviors initiated in HAZ are difficult to propagate along the grain boundary. Otherwise, in the high Si content alloy, there are a large number of residual eutectic phases formed as films at the grain boundary, leading to easy crack propagation.

Besides, the laser welding technique shows good compatibility to other welding methods, which has been systematically studied. The laser welding/brazing technology is good at combining fusion welding of dissimilar materials with low melting point metals and brazing of dissimilar materials with high melting point metals, and it has been applied to joining the following dissimilar materials: magnesium/titanium, aluminum/copper, magnesium/steel, and aluminum/steel (Wallerstein et al., 2021a; Wallerstein et al., 2021b; Wang et al., 2021b; Krisam et al., 2022; Xia et al., 2022). However, few researches have been done to systematically study on the properties of high silicon aluminum alloy by laser welding.

Therefore, in this paper, the properties of high silicon aluminum alloys using a LPKF laser welding machine are comprehensively studied. The alloy materials are Al-50wt.%Si shell and Al-27wt.%Si cover plate. By comparing the surface morphology, microstructure, and microhardness under different welding process parameters, the influence of power and pulse width on the joints was systematically analyzed.

2 Materials and methods

2.1 Materials

High silicon aluminum materials prepared by jet deposition method were selected as experimental materials, where aluminum silicon alloy containing 50% silicon content (mass fraction) is selected as the shell, the cover plate is made of silicon aluminum alloy with 27% silicon content. The main physical properties of high silicon aluminum are shown in Table 1. From the table, it can be seen that, with the improvement of silicon content, the coefficient of thermal expansion (CTE), density, and thermal conductivity, and yield strength decrease, while the elasticity module increase, as the silicon fillers are hard, light, and low conductive materials.

Figure 1 shows mechanical structure of the laser welding samples. The shell and the cover plate contact with each other using lap structure. A block was put on the cover plate to apply load to fix the plate against thermal deformation during welding process. A LPKF equipment was used to perform the laser welding process in an argon atmosphere protected glove box.

2.2 Analysis method

The morphology of joints was observed by a Leica optical microscope (OM). The properties of laser welding samples were analyzed by metallographic analysis. Firstly, the laser welding samples were cut by a wire cutting machine. Secondly, the samples were encapsulated with epoxy and treated by mechanical polishing with SiC abrasive sandpaper (50#, 200#, 800#, 1,000#, and 2,000#), and then the cross-sectional samples were polished with a .1 μm diamond suspension to eliminate surface scratches. The microstructure of prepared samples was observed by a TESCAN Vega three scanning electron microscope (SEM) equipment at 10 kV–20 kV. Vickers microhardness tester was used to test the microhardness of the welded joints. The loading load was 2.942 N and the loading time was 10 s. During the test, the joints were tested horizontally and longitudinally.

3 Results and discussion

3.1 The surface morphologies of joints

A LPKF P02500 laser welding equipment was used to carry out the study. The main two parameters are power and pulse width. The power is 1,300 W, 1,500 W, 1,800 W, 2,000 W, and 2,300 W respectively, while the pulse width is 3 ms, 4 ms, and 5 ms, respectively.

Figure 2 shows the surface morphologies of laser welding joints. It can be seen that the surface morphologies of all of the prepared joints are good, and the fish scale patterns on the joint surface are uniform and smooth, indicating that laser welding parameters selected in this study makes the high silicon aluminum have good fluidity during welding process. The forming of fish scale pattern is because of the weld solidification sequence during laser welding. The pulsed laser energy output is intermittent. When the laser beam moves forward, the pulsed laser energy will melt not only the base materials, but also the tail of the adjacent welding spot. Therefore, the welding seam is not

TABLE 1 The properties of high silicon aluminum alloys.

Si content (mass fraction)	C (%)TE ($\times10^{-6}$ K^{-1})	Density ($g{\cdot}cm^{-3}$)	Thermal conductivity ($W{\cdot}m^{-1}{\cdot}K^{-1}$)	Yield strength (MPa)	Elasticity module (GPa)
27	16.0	2.6	177	183	92
50	11.0	2.5	149	125	121

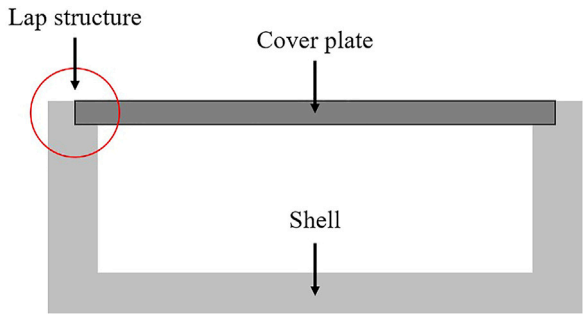

FIGURE 1
The mechanical structure of laser welding samples.

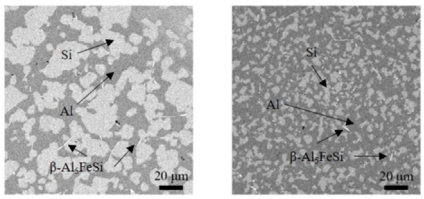

FIGURE 3
(A) The SEM image of Al-50wt.%Si alloy, **(B)** The SEM image of Al-27wt.%Si alloy.

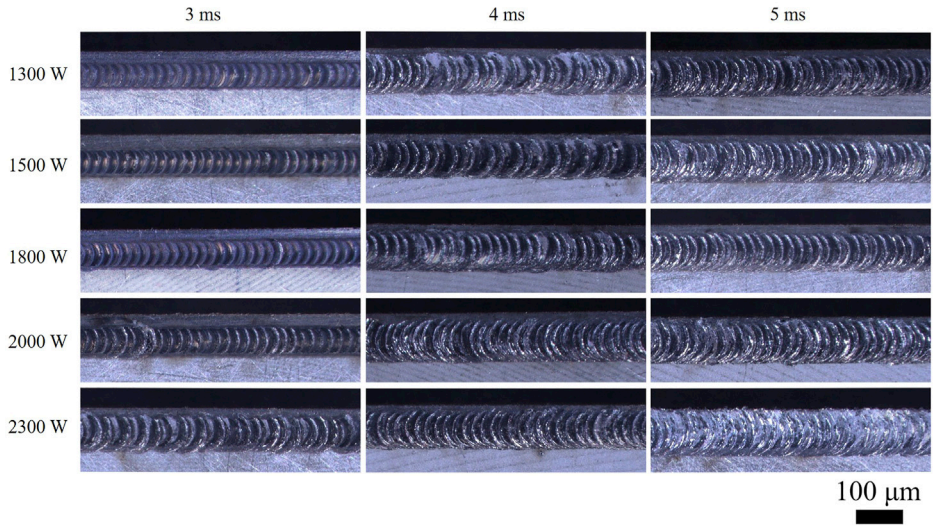

FIGURE 2
The surface morphologies of joints.

smooth and has obvious pulse characteristics in front, and the welding spot texture is large and clear. The arrangement is dense and neat.

In Figure 2, a clear phenomenon is shown, the influence of power on joint width is minor than that of pulse width on joint width. For example, the joint width at parameter of 1,300 W and 3 ms is about 49.4 μm. When the power is 2,300 W and pulse width is 3 ms, the joint width is 57.4 μm. However, with parameters of 5 ms and 1,300 W, the joint width reaches at 84 μm. In summary, higher pulse width will form wider joint, while the power has slight influence on welding width. Although the higher power can increase the input energy, the simply increasing the power cannot obviously extend size of the welding spot, as the high thermal conductive base materials owns the ability of quick heat dissipation. By contrast, when the laser pulse width is enhanced, there will form larger welding spot, causing wider melting area.

3.2 The microstructures of joints

Figure 3 shows the material microstructure characteristics of the Al-50wt.%Si and Al-27wt.%Si high silicon aluminum alloys. The light area in SEM image is the Si particle, part of which is skeleton-like and

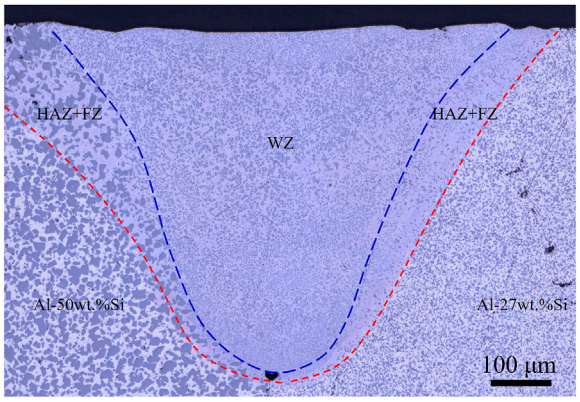

FIGURE 4
The typical cross-sectional SEM image of joint.

part of which is granular, while the dark area in SEM image is the Al phase. The average diameter of silicon particles is about 25 μm in the Al-50wt.%Si high silicon aluminum alloy, while most of the silicon particles are distributed between 10 μm and 40 μm. For the Al-27wt.% Si high silicon aluminum alloy, the size of silicon particles variates from 2 μm to 10 μm. The silicon particles are diffusely distributed in the Al matrix and two phases mix evenly, which is beneficial for improving the thermal conductivity of the material and reducing the linear CTE. Besides, β-Al_5FeSi phase is distributed in a small amount between Al phase and Si phase. According to the phase diagram of Al-Si binary alloy, aluminum alloys of Al-27wt.%Si and Al-50wt.%Si are hypereutectic alloys, and their solidification structure is mainly composed of primary silicon and Si-Al eutectic, in which Al-Si eutectic is composed of α-Al + Si. However, the solubility of aluminum in silicon is very small at room temperature. Therefore, the eutectic silicon in Si-Al eutectic can be regarded as pure silicon (Chen et al., 2014).

Figure 4 shows the typical material microstructure characteristics of the joints. Usually, the joint can be divided into weld zone (WZ), fusion zone (FZ), and HAZ. Because laser welding has the characteristics of fast welding speed, high energy density, and small heat input, HAZ of laser welding joint is small, which is an important advantage of laser welding compared with other welding techniques. From Figure 4, it can be seen that the thickness of HAZ and FZ adjacent to the Al-50wt.%Si base material increases from 20 μm to 150 μm, and the highest value is near the surface of joint. When the HAZ and FZ near the Al-27wt.%Si base material, the thickness variation of HZA and FZ is from 20 μm to 110 μm. As shown in Figure 4, the microstructure of FZ is finer than that of both of Al-50wt.%Si and Al-27wt.%Si base materials, and the microstructure is mainly fine equiaxed crystal. Based on the analysis of the above results, it is believed that many complex metallurgical reactions occur in the molten pool at high temperature step in a very short time. Also, these changes will directly determine the microstructure, mechanical properties, and performance of the joints. Compared to other conventional welding processes, the pulsed laser beam energy is low and has less heat input to welding joints. Moreover, the high thermal conductivity of high aluminum alloys accelerates the cooling rate of the molten pool and leads to quick temperature drop. The residence time at high temperature and the grain growth time are shortened. Additionally, the homogeneous nucleation of silicon particles in melting pool makes that the microstructure of FZ is finer and more uniform than the base materials.

Under normal conditions, one major defect in aluminum alloy welding is the hydrogen porosity, which is characterized by sphericity, small size, and large number. The difference in the solubility of hydrogen in liquid aluminum and solid aluminum results in the formation of hydrogen pores. During laser welding of high silicon aluminum alloys, some hydrogen atoms escape due to the sharp heating and cooling. It is generally believed that the formation process of hydrogen stomata has three stages: hydrogen accumulates to form small hydrogen stomata; hydrogen pores grow to form bubbles; bubbles float up and escape. Due to the large thermal conductivity of Si-Al materials, the condensation is fast. Meanwhile, the viscosity of molten aluminum material is large and the bubble radius is small, so the floating speed of hydrogen bubbles is small in the solution pool. In summary, the low rising speed, the short rising time, and the relative long path make it difficult for bubbles to rise to the surface and escape, so some bubbles are frozen in the FZ.

Besides, a large number of cracks usually pass through the silicon particles and aluminum matrix. This is because the stress state of some silicon particles changed significantly during the welding cold-heat cycle, which changed sharply from compressive stress to tensile stress, leading to the fracture of silicon particles. In the part near the molten pool, the silicon was filled with molten aluminum after rupture, so the crack did not expand further. However, the material near the base material zone has high silicon content and is affected by welding heat. The aluminum matrix does not melt. Under the action of tensile stress during the cooling process, a large amount of brittle silicon breaks, expands, and passes through the aluminum matrix, resulting in macroscopic cracks in the HAZ. In the crack propagation, the propagation trajectory is along the boundary of silicon particles or penetrates the silicon particles. On the one hand, the silicon particles of Al-Si alloy have sharp edges and corners, which are easy to produce stress concentration, thus piercing the phase and forming cracks. On the other hand, the silicon particles are poor in plasticity and easy to fracture under the influence of stress.

According to the above analysis, the main defects in laser welding joints of high silicon aluminum alloy are pores and cracks. Thus, to forbid obvious hydrogen pores and cracks, the laser welding speed is setting at 3 mm/s~5 mm/s. As shown in Figure 5, although the hydrogen pores and cracks are difficult to avoid, both defects do not form in prepared samples in this research, due to reasonable welding parameters. As the welding thermal cracks are the main factor of air tightness problem, it can speculate that the samples prepared in this study own high resistance to air loss. As shown in Figure 5, the joint depth is 41.1 μm at power of 1,300 W and pulse width of 3 ms. Just increasing the pulse width to 5 ms does slightly increase the joint depth, which is 49.6 μm. But just enhancing the input power to 2,300 w does obviously improve the joint depth to 125.2 μm. Therefore, the laser power is the key parameter to control the joint depth.

3.3 Hardness of joints

As shown in Figure 6A, the microhardness test was carried out along the horizontal direction of joint, the points were successively taken through the cover plate, the HAZ near cover plate, the FZ near cover plate, the WZ, the FZ near the shell, the HAZ near shell, and the

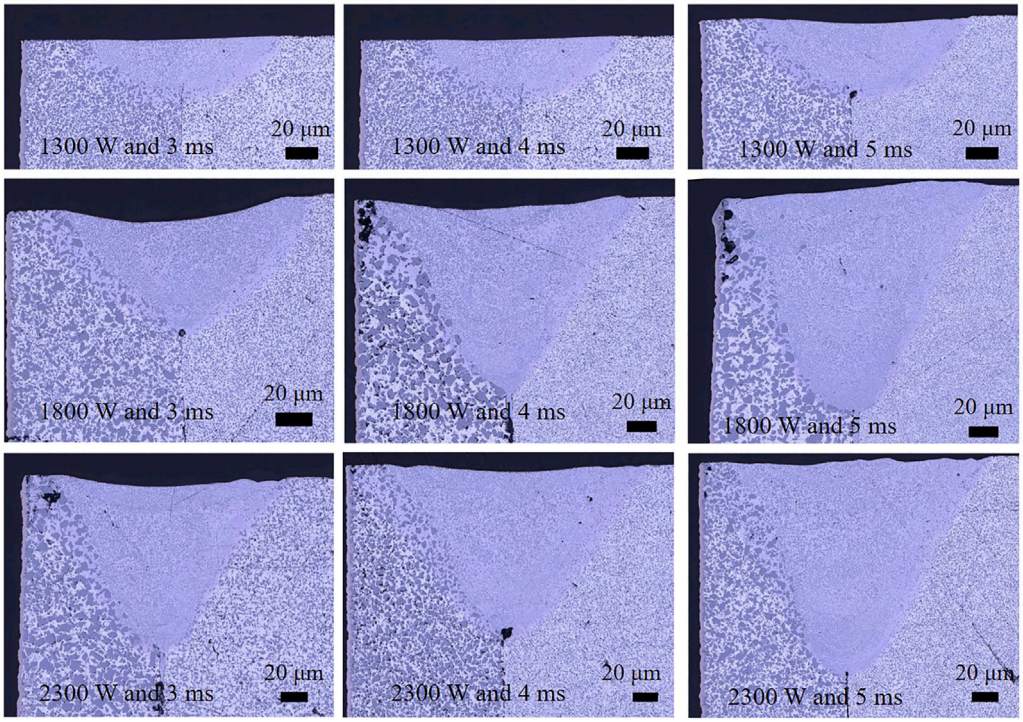

FIGURE 5
The microstructure of joints at different parameters.

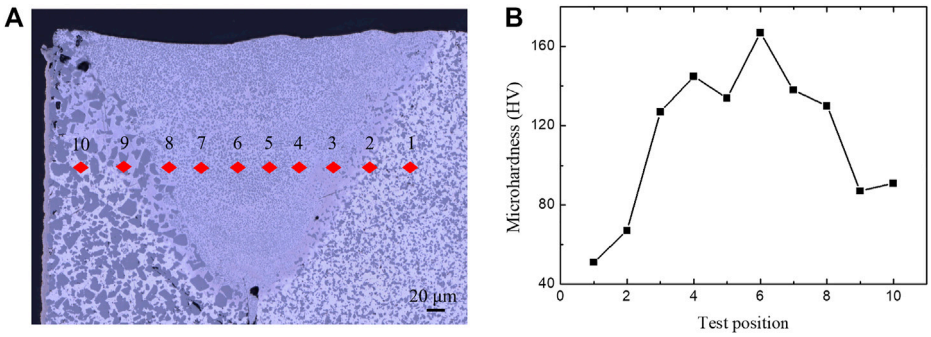

FIGURE 6
(A) Test position of horizontal microhardness of the joint, **(B)** microhardness testing results.

shell. When the points were taken, multiple samples were tested and the average value was calculated. After comparing the testing results in Figure 6B, it is found that the microhardness of two parts is different due to the different Si contents of the cover plate and the shell, which are Al-27wt.%Si and Al-50wt.%Si, respectively. The microhardness of the cover plate is 51 HV, while the microhardness of the shell is 91 HV. Additionally, it can be seen from the microhardness distribution line diagram, the microhardness gradually increases from the FZ to the WZ, and the microhardness closer to the center of WZ is higher. Among them, the microhardness of the FZ is about 130 HV, and the microhard-ness of the WZ is about 167 HV. The results show that laser welding could significantly improve the joint microhardness. Because the microstructure of the WZ in the center of the joint is fine, the microhardness is higher. Besides, the Si particles are distributed evenly in joints, the microhardness measurement results in the weld retain a slight fluctuation.

In Figure 7A, the microhardness test was carried out along the center line of the joint longitudinally, and points were successively taken from the upper surface of the joint to the bottom of the joint. It can be seen from Figure 7B, from the top surface to the bottom of the joint, the microhardness value is relatively stable, but the overall fluctuation is slightly. The test position near the joint center has the highest hardness value, and the microhardness value is about 165 HV, followed by the part near the top surface, whose

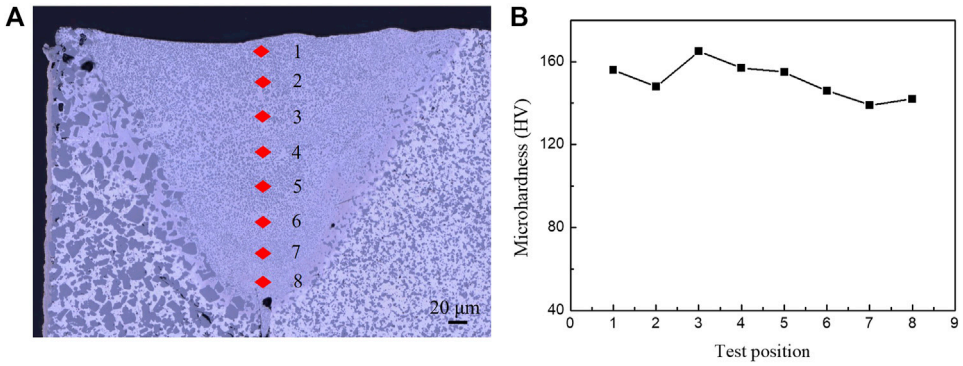

FIGURE 7
(A) Test position of longitudinal microhardness of the joint, **(B)** microhardness testing results.

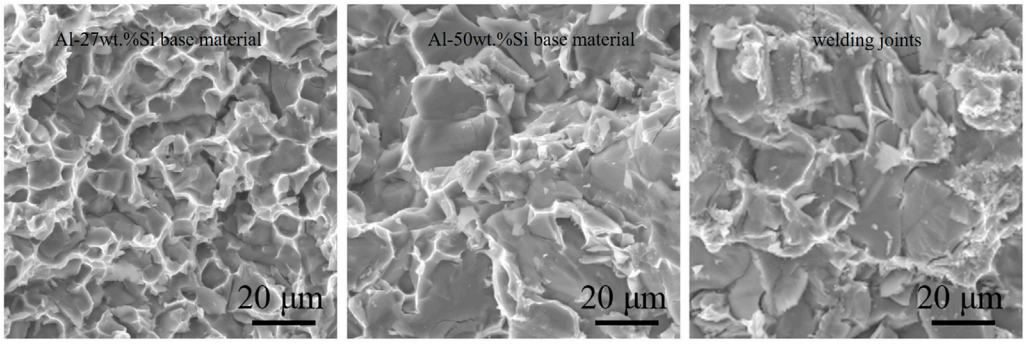

FIGURE 8
The fracture morphologies of base materials and welding samples.

microhardness value is about 156 HV. The lowest microhardness value is the joint bottom with microhardness of about 139 HV. In the center zone, the microstructure is the primary silicon and aluminum silicon eutectic tiny grains, so the hardness is generally on the high level. The position at the bottom of the joint is close to the joint gap between the shell and the cover plate, where there are many defects, such as pores. Although the defects are efficiently reduced, the existence of pores will affect the mechanical properties of the surrounding zone to some degree, causing microhardness decrease.

3.4 Tensile properties of joints

The tensile tests were carried out to the Al-27wt.%Si and Al-50wt.%Si base materials and welding samples. The experiments were conducted using a Instron mechanical test machine. The experimental speed was .05 mm/min and the standard distance was 50 mm. To minimize the experimental errors, five samples were selected to each group, the tensile strength and extension rate were the average value of five samples. The Al-27wt.%Si and Al-50wt.%Si base materials are the control samples and welding samples are the experimental samples. The tensile strengths of the Al-27wt.%Si and Al-50wt.%Si samples are 189.3 MPa and 218.8 MPa, respectively, and the extension rate of Al-27wt.%Si and Al-50wt.%Si samples are 6.2% and 11.4%, respectively. As the grain size of the Al-27wt.%Si base material is smaller than that of the Al-50wt.%Si base material, the mechanical strength and elongation of the former material is greater than that of the latter material, which has been proved in the above research content. By comparison, the tensile properties of laser welding samples and Al-50wt.%Si base materials are almost the same. The welding samples have tensile strength of 187.5 MPa and extension rate of 6.1%.

Figure 8 shows the representative fracture morphologies of base materials and welding samples. For the Al-27wt.%Si base materials, which have less silicon content, relatively fine dimples exist in the fracture location, indicating that the fracture mechanism is ductile fracture. For the Al-50wt.%Si base materials, the crack is splitting through the silicon particles, resulting in brittle fracture. In summary, the less silicon content and smaller silicon particle size could enhance the mechanical strength and elongation property of silicon-aluminum alloy. By observing the welding samples, the fracture locates at the Al-50wt.%Si base material near the joints, and the fracture morphology is similar to the morphology of the Al-50wt.%Si samples. In this study, the spot of the pulsed laser beam is small, and the residual stress is small, effectively reducing the deformation and restraint during laser welding. Additionally, few of pore forms in the joints by pulsed laser welding, and the grain size of welding sample is smaller than both base materials. Thus, the joints of the welding samples are stronger than the base materials. By contrast, the Al-50wt.%Si base material is the

weakest part in the welding samples, and the uneven surface leads to stress concentration. Thus, the fracture initiates at the Al-50wt.%Si base material near the welding joint.

4 Discussion

The current study investigated the properties of high silicon aluminum alloys by laser welding. Here, it conducted experiments in a wide range of welding power and pulse width. The conclusion of this study can be drawn as follows:

(1) The most suitable welding speed is 3–5 mm/min, which can significantly reduce the hydrogen pores and cracks in laser welding joints.
(2) The key parameters of laser welding to control the quality of joints are power and pulse width, while the former one is mainly controlling the joint width and the latter one is mainly changing the joint depth.
(3) Along the horizontal direction of laser welding joints, the microhardness goes up firstly and then goes down, with the highest microhardness of 167 HV in the WZ. Because the laser welding technique could produce uniform microstructure of joints, the micro-hardness of joints is relatively stable and slightly fluctuates along the longitudinal direction.
(4) The tensile strength and the extension rate of welding sample is almost the same with that of Al-50wt.%Si base material, due to the microstructure refinement effect of pulsed laser welding.

Data availability statement

The original contributions presented in the study are included in the article/Supplementary Material, further inquiries can be directed to the corresponding authors.

Author contributions

Conceptualization, DY; methodology, DY; software, YH; validation YH; investigation, DY; data curation, YH; writing—original draft preparation, DY; writing—review and editing, YH; supervision, DY; project administration, DY. All authors have read and agreed to the published version of the manuscript.

Conflict of interest

DY and YH were employed by Guobo Electronics Co., Ltd.

Publisher's note

All claims expressed in this article are solely those of the authors and do not necessarily represent those of their affiliated organizations, or those of the publisher, the editors and the reviewers. Any product that may be evaluated in this article, or claim that may be made by its manufacturer, is not guaranteed or endorsed by the publisher.

References

Abbaschian, L., and Lima, M. S. F. D. (2003). Cracking susceptibility of aluminum alloys during laser welding. *Mater. Res.* 6 (2), 273–278. doi:10.1590/s1516-14392003000200024

Aktarer, S. M., Sekban, D. M., Saray, O., Kucukomeroglu, T., Ma, Z. Y., and Purcek, G. (2015). Effect of two-pass friction stir processing on the microstructure and mechanical properties of as-cast binary Al–12Si alloy. *Mat. Sci. Eng. A* 636, 311–319. doi:10.1016/j.msea.2015.03.111

Chen, X. Y., Li, Y. X., and Liu, J. Y. (2014). The fabrication of high silicon-aluminum composites and the thermal conductivity. *Adv. Mat. Res.* 941–944, 288–293. doi:10.4028/www.scientific.net/amr.941-944.288

Hou, J., Li, R., Xu, C., Li, T., and Shi, Z. (2021). A comparative study on microstructure and properties of pulsed laser welding and continuous laser welding of Al-25Si-4Cu-Mg high silicon aluminum alloy. *J. Manuf. Process.* 68, 657–667. doi:10.1016/j.jmapro.2021.05.064

Hu, M., Wang, T., Fang, H., and Zhu, M. (2021). Modeling of gas porosity and microstructure formation during dendritic and eutectic solidification of ternary Al-Si-Mg alloys. *J. Mat. Sci. Technol.*,76 76–85. doi:10.1016/j.jmst.2020.11.008

Jia, S. Q., Jiang, X., He, J. J., Zhu, X. G., and Chen, M. (2011). Effect of Al-Si solder on properties of dissimilar aluminum alloy weld by electron beam welding. *Nonferrous Met. Extr. Metall.* 07, 30–34. doi:10.1016/j.jmrt.2021.09.053

Krisam, S., Becker, H., Silvayeh, Z., Treichel, A., Domitner, J., and Povoden-Karadeniz, E. (2022). formation of long-range ordered intermetallic η''' phase and the involvement of silicon during welding of aluminum-steel sheets. *Mat. Charact.* 187, 111862. doi:10.1016/j.matchar.2022.111862

Kun, Y. U., Li, S. J., Chen, L. S., Zhao, W. S., and Li, P. F. (2012). Microstructure characterization and thermal properties of hypereutectic Si-Al alloy for electronic packaging applications. *Trans. nonferr. Metal. Soc.* 226, 1412–1417. doi:10.1016/s1003-6326(11)61334-4

Kutsuna, M., Shido, K., and Okada, T. (2003). Fan shaped cracking test of aluminum alloys in laser welding. *Proc. SPIE-The Int. Soc. Opt. Eng.* 4831, 230–234. doi:10.1117/12.497901

Liu, Y., Wei, S., Zuo, T., Ma, Z., and Fan, J. (2012). Preparation and microstructure evolution of powder metallurgy 70%Si/Al composites. *Chin. J. Rare Metal.* 1, 1–10. doi:10.3969/j.issn.0258-7076.2012.06.005

Meng, X. C., Huang, Y. X., Cao, J., Shen, J. J., and dos Santos, J. F. (2021). Recent progress on control strategies for inherent issues in friction stir welding. *Prog. Mat. Sci.* 115, 100706. doi:10.1016/j.pmatsci.2020.100706

Quazi, M. M., Fazal, M. A., Haseeb, A. S. M. A., Yusof, F., Masjuki, H. H., and Arslan, A. (2015). Laser-based surface modifications of aluminum and its alloys. *Crit. Rev. Solid State* 41, 106–131. doi:10.1080/10408436.2015.1076716

Wallerstein, D., Salminen, A., Lusquiños, F., Comesaña, R., Val, García J. D. V., Rodríguez, A. R., et al. (2021). Recent developments in laser welding of aluminum alloys to steel. *Metals* 11, 622. doi:10.3390/met11040622

Wallerstein, D., Solla, E. L., Lusquiños, F., Comesaña, R., Val, J. D., Riveiro, A., et al. (2021). Advanced characterization of intermetallic compounds in dissimilar aluminum-steel joints obtained by laser welding-brazing with Al-Si filler metals. *Mat. Charact.* 179, 111345. doi:10.1016/j.matchar.2021.111345

Wang, J., Fu, X., Zhang, L., Zhang, Z., Liu, J., and Chen, S. (2021). A short review on laser welding/brazing of aluminum alloy to steel. *Int. J. Adv. Manuf. Technol.* 112, 2399–2411. doi:10.1007/s00170-021-06607-4

Wang, Y., Yang, X., Shi, S., Wu, Z., Han, R., and Qi, H. (2021). Laser welding 6061 aluminum alloy with laser cladding powder. *J. Laser Appl.* 33, 022006. doi:10.2351/7.0000217

Wu, Q. S., He, J. S., and Feng, J. C. (2006). Characteristic parameter describing appearance of aluminum alloy weld in electron beam welding. *Trans. China Weld. Institution* 27, 1–4. doi:10.1016/j.jestch.2022.101093

Xia, H., Li, L., Tan, C., Yang, J., Li, H., Song, W., et al. (2022). *In situ* SEM study on tensile fractured behavior of Al/steel laser welding brazing interface. *Mat. Des.* 224, 111320. doi:10.1016/j.matdes.2022.111320

Zhang, Q., Jiang, L., and Wu, G. (2015). Microstructure and thermo-physical properties of a SiC/pure-Al composite for electronic packaging. *J. Mat. Sci. Mat. Electron.* 25, 604–608. doi:10.1007/s10854-013-1474-x

Zhao, P., Liu, J., and Chi, Z. (2014). Effect of Si content on laser welding performance of Al-Mn-Mg alloy. *Trans. Nonferrous Metals Soc. China* 24, 2208–2213. doi:10.1016/s1003-6326(14)63334-3

Zhong, G., An P., Mao, Y. W., Li, S. Z., Zhong, G., Wu, S. S., et al., (2010). Microstructure and properties of high silicon aluminum alloy with 2% Fe prepared by rheo-casting. *Trans. nonferr. Metal. Soc.* 20, 1603–1607. doi:10.1016/s1003-6326(09)60346-0